Publishing House
AKAPIT

COMPUTER METHODS IN MATERIALS SCIENCE

Informatyka w Technologii Materiałów

Vol. 12, 2012, No. 3

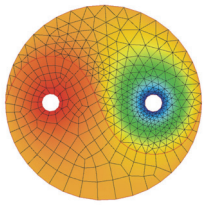

MICRO SCALE MODELLING OF STRESS AND STRAIN PARTITIONING IN HIGH STRENGTH DUAL PHASE STEELS

ALIREZA ASGARI[1*], HASSAN GHADBEIGI[2], CHRISTOPHE PINNA[2], PETER D. HODGSON[3]

[1] School Of Engineering, Deakin University, Victoria, 3216, Australia
[2] Department Of Mechanical Engineering, The University Of Sheffield, Sheffield S1 3jd, Uk
[3] Institute For Frontier Materials, Deakin University, Victoria, 3216, Australia
**Corresponding author: alireza.asgari@research.deakin.edu.au*

Abstract

Multiscale modelling of stress and strain partitioning in Dual Phase (DP) steel was carried out using both realistic microstructure-based Representative Volume Element (RVE) models as well as stochastic microstructures generated by Monte Carlo (MC) method. The stochastic microstructure models were shown to resemble that of realistic microstructures, enabling research on the specific aspects of the microstructure that could be difficult to control and study during experimental work. One such feature of the realistic microstructures studied in this work was the grain size and microstructure morphology. The microstructures were generated with varying average grain sizes while all other parameters, such as boundary conditions, material properties and volume fractions of martensite and ferrite were kept constant. It is found that the effect of grain size is much more pronounced during the initial localisation of the plastic deformation at and around the interface of the phases. In addition, the decrease in ductility and increase in strength of the DP steels are directly related to the refinement of grain sizes of each phase and the stress-strain partitioning in between them.

Key words: Realistic microstructure, RVE, Monte Carlo simulation, grain size, Dual Phase steel

1. INTRODUCTION

Research on Advanced High Strength Steels (AHSS) is stimulated by the need to understand (and benefit from) the profound microstructural effects of these materials and achieve the desired balance between the strength and durability. The so called third generation AHSS steels are expected to fill the gap between the ideal balance of the strength, ductility and the complex and costly manufacturing issues (Wagoner, 2006). Problems involved in the forming of AHSS are very similar to those encountered in the forming of conventional steels. However, the complex microstructural phenomena in AHSS accentuates some of the manufacturing issues such as higher loads on presses and tools, greater energy requirements and increased need for springback compensation and control. During forming process, AHSS sheets have greater tendency to wrinkle because of the lack of adequate binder force and often a reduction in sheet thickness. Dual Phase (DP) steel is a well-studied AHSS with numerous research and applied works carried out on its forming, springback and crash simulation and experiments (Al-Abbasi & Nemes, 2003; Jacques et al., 2007; Lani et al., 2003; Lani et al., 2007; Nygards & Gudmundson, 2002; Rashid, 1981; Saleh & Priestner, 2001; Sun, X. et al., 2009a; Wagoner, 2006). The microstructure of DP steel contains a soft ferrite matrix with hard martensite inclusions and in some cases small amounts of retained austenite or other phases (Zaefferer et al.,

 ISSN 1641-8581

2004). DP steels have high tensile strengths as well as moderate total elongations, excellent for automotive applications such as cold-pressed wheel rims, B-pillars or other body-in-white parts (De Cosmo et al., 1999; Konieczny, 2001; Konieczny et al., 2001). Due to unique combination of soft and hard phases in DP steel, the microstructural configuration influences the stress-strain curve. In other AHSS such as Transformation Induced Plasticity (TRIP), phase transformation plays a significant role too but the composite effect of microstructural features remains to be similar to that of DP steel. In DP steel, the yield stress is determined by the onset of the plastic flow in the soft phase, ferrite. At this stage, martensite is still in the elastic region. With higher applied stress, the material exhibits exceptional work hardening behaviour. Therefore, strain partitioning occurs in the two phases such that in the soft phase the strain and in the hard phase the stress remains above the mean value of the composite DP steel. The easiest and straight forward way to explain this behaviour is by using the mixture rule of composite structures (Hulka, 2003). However, the simple additive rule of mixtures is only valid for the axial components of flow stress and strain of the phases (Dietrich et al., 1993). The partitioning of stress and strain between the ferrite and martensite phases are required to be known to calculate the flow behaviour of the dual phase. For a two phase composite structure, this partitioning can be characterised by the ratio *m* defined in figure 1 as the slope of the tie line which joins correlated stresses and strains in the soft ferrite (F) and hard martensite (M) and the composite structure, DP steel (Dietrich et al., 1993). Corresponding states of soft and hard phase are essentially defined by the time step of the micro-scale model.

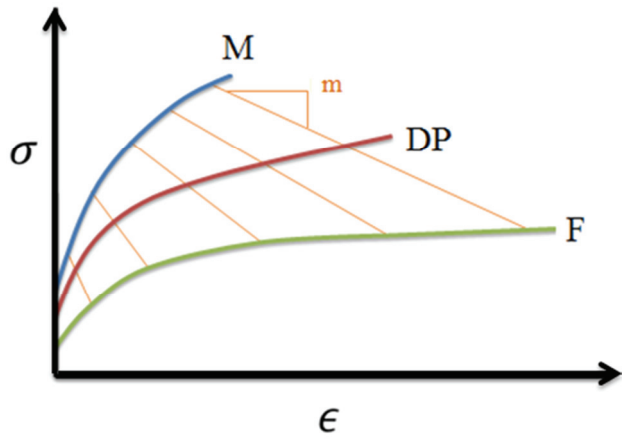

***Fig. 1**. Schematic stress-strain relationship between hard phase (martensite), soft phase (ferrite) and the composite structure (DP steel) described in terms of m slope of the line joining corresponding state in the two phases.*

Shown in figure 1, at any given point in time, the hard phase (M) could experience higher stresses and lower deformation than what will be experienced by the soft phase (F).

Instead of the simple rule of mixtures, a realistic microstructure modelling technique can be used to investigate stress and strain partitioning in DP steels (Asgari et al., 2009). In this multiscale context, the finite element modelling is employed to provide a predictive capability for microstructure design of DP steels in which material properties are resulted from only few input parameters relevant to the constituent phases. In recent years, the realistic microstructure modelling technique has been greatly exploited to analyse and study the different micromechanical features of DP steels and other AHSS. Sun and co-workers have performed micromechanical failure analysis based on the actual microstructure of DP steels (Sun, X. et al., 2009a). In their study, heterogeneity of the microstructure is used to initiate the plastic localisation due to the incompatible deformation between hard martensite and soft ferrite. The ultimate failure of the material is therefore dictated by the initial microstructural inhomogeneity which translates into coalescence of the highly strained regions in the RVE (Sun, X. et al., 2009a). In a series of similar works (Choi et al., 2009a; 2009b; Choi et al., 2010; Cong et al., 2009; Soulami et al., 2010; Soulami et al., 2011; Sun, X. et al., 2009a; Sun, X. et al., 2009b), they have used realistic microstructure-based modelling to study the effect of various parameters and features on ductility and failure of DP and TRIP steels. In one example, Sun et al. used various microstructure-based models with different volume fraction of martensite and varying distributions of micro voids to study the ductility of the DP steels (Sun, X. et al., 2009b). The effect of pre-existing micro voids on reduction of ductility were found to be more pronounced when the volume fraction of martensite was less than 15%. When the volume fraction of martensite is above 15%, the overall ductility is found to be influenced by the incompatible deformation between martensite and ferrite. The size of Optical Micrographs (OMs) that Sun and co-worker have studied range between 51 to 92 μm. Their models are considered to be in the state of plane stress with displacement boundary conditions defined to simulate the uniaxial tensile loading along the rolling direction defined as x direction in the RVEs. The right side of RVE is displaced in x direction, the left side is fixed in x direction while both sides are left free in y direction. The

macroscopic engineering stresses are calculated by using the reaction force of the RVE in the x direction divided by the initial area and engineering strains are calculated by dividing the displacement of the right edge with the initial length of the model. This method of setting up and running an RVE model has two drawbacks. First, the engineering strain is prescribed by the user and second, the effect of various initial sizes of the RVEs, which is explicitly embedded in the results, is ignored. Furthermore, the application of displacement boundary condition, as well as traction boundary conditions are shown not to be suitable to represent a microstructure statistically (Kouznetsova, 2002). It is well known in the literature that periodic boundary conditions are much more representative when an RVE is being used, even if the microstructure is not physically periodic (Terada et al., 2000; Van der Sluis et al., 2000). When displacement or traction boundaries are used the sampling size of the RVE must be significantly increased to include enough microstructural information into simulation (Kouznetsova, 2002).

In this paper, we use periodic boundary conditions on RVEs that are created from the realistic microstructure as well as RVEs that are created stochastically with only one varying parameter, the grain size. The microstructures that are created using Monte Carlo simulations of grain growth significantly resemble the actual micrographs of DP steels, thus enabling us to study the effect of grain size variation and sampling of microstructure information while all other parameters and features in the multiscale models are kept constant.

2. METHODOLOGY

2.1. Realistic microstructure-based RVEs

Two commercial grade steels of DP590 and DP1000 were selected for this study. The chemical composition and volume fraction of constituent phases for the two DP steels are shown in table 1.

The experimental results on the evolution of the local stress and strain of in-situ tensile tests of DP1000 steel using Digital Image Correlation (DIC) technique are documented by Ghadbeigi et al. (2010). Similarly, the experimental results on uniaxial tensile test and stretch forming of DP590 are established by Nikhare et al. (2010). The realistic microstructure models of these steels were generated using Optical Micrographs) OMs based on a procedure explained in more details in a previous study (Asgari et al., 2009). The material properties of ferrite and martensite were defined by using the stress-strain curves of each constituent phase as an elasto-plastic material (figure 2). The stress–strain curves of each phase were obtained from experimental measurements of Delannay and co-workers as presented in Delannay et al. (2005)

The models are assumed to be in a quasi-static state, where inertia effects are ignored. The von Mises yield condition is assumed for martensite and ferrite given by

$$f = \sigma - \sigma_Y \tag{1}$$

The equivalent stress, σ, is given by

$$\sigma = \sqrt{\frac{3}{2}\,\sigma'_{ij}\sigma'_{ij}} \tag{2}$$

with the deviatoric stresses $\sigma'_{ij} = \sigma_{ij} - \sigma_{kk}/3$. The yield stress σ_Y is taken to be a function of the equivalent plastic strain to describe the isotropic hardening behaviour of the single phases, as shown in figure 2. In a previous study (Asgari et al., 2009), we have developed a sub-volume homogenisation method in which a finite number (r_n) of RVEs could be selected and the macroscopic stress components were found by a global averaging scheme over all selected RVEs. In this work the value of $r_n = 1$ was used, and the macroscopic stress was found by a volume averaging over the domain of the selected RVE. The same number of nodes was used on the left and right sides as well as top and bottom of the RVEs and the periodic boundary conditions were prescribed on each model to ensure a representativeness of RVE is achieved.

Table 1. *Chemical composition of selected commercial DP steels from (Ghadbeigi et al., 2010; Nikhare et al., 2010).*

Steel Grade	Thickness	Chemical composition, wt%							
		C	Mn	Si	Al	Nb	Cr	V	Ni
DP590	1.97 mm	0.069	1.410	1.040	0.022	0.011	-	-	-
DP1000	1.5 mm	0.152	1.53	0.474	-	-	0.028	0.011	0.033

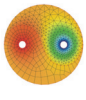

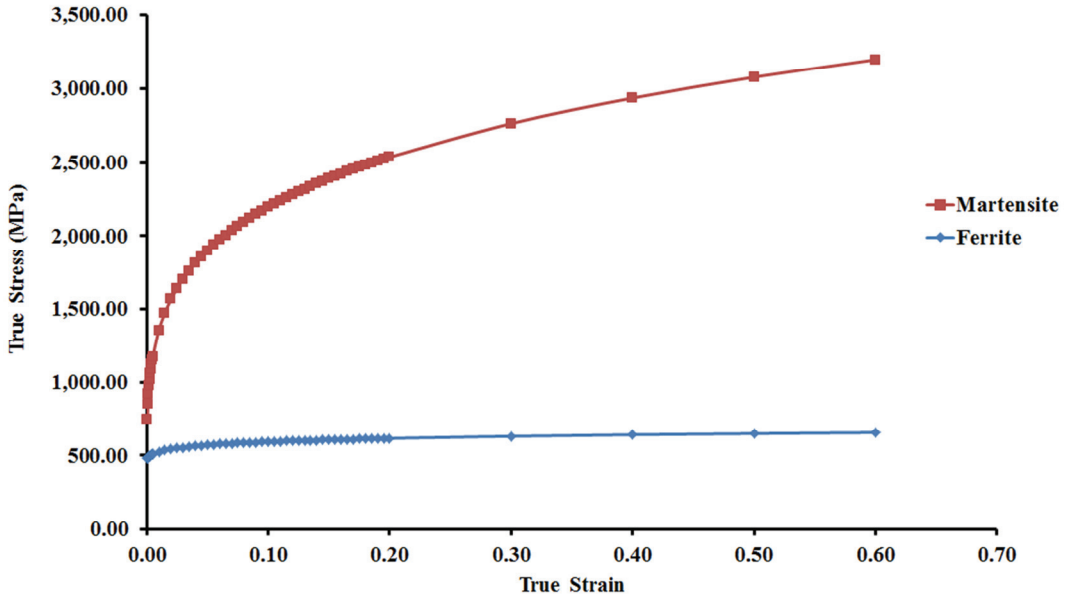

Fig. 2. *Stress–strain curves of single phases used in the microscale model.*

2.2. Stochastic RVEs created by Monte Carlo grain growth simulation

To study the effect of microstructure morphology and grain size of DP steel while all other parameters are kept constant, we use a stochastic Monte Carlo simulation method to control the static grain growth and generate initial microstructures. These microstructures are then meshed and studied with the same technique described in previous section for the realistic micrographs of DP steel.

A review of MC Potts model is provided by (Miodownik, 2002), and here we describe the steps relevant to the generation of microstructures in this work. The microstructures are generated from a random distribution of the cubic 2D lattices. The random state was reset at the beginning of each microstructure generation therefore resulting in microstructures that have same random distribution with the only controlled difference being the grain size due to initially prescribed lattice sizes. The lattice sizes were chosen to be in the range of 1/30 to 1/480 µm. Here we use Monte Carlo Q-state Potts method with modifications described by (Ming Huang et al., 2006; Zheng et al., 2006) to simulate the recrystallization from these initial random lattice distributions. In this type of MC Potts model, the grain growth is controlled by the grain boundary energy inside each phase as well as the interfacial energy between two phases. A two dimensional triangular domain of 1x1 mm is considered in which NxN lattices are dispersed. The energy of the whole system is found by its Hamiltonian defined as

$$H = \frac{1}{2}J_{MF}\sum_{i=1}^{N^2}\sum_{j=1}^{K}\left(1-\delta_{S_iS_j}\right) + \frac{1}{2}J_M\sum_{i=1}^{N_M}\sum_{j=1}^{K_M}\left(1-\delta_{Q_iQ_j}\right) + \frac{1}{2}J_F\sum_{i=1}^{N_F}\sum_{j=1}^{K_F}(1-\delta_{P_iP_j}) + N_FE_F + N_ME_M \quad (3)$$

where N^2 is the total number of lattice sites, N_F and N_M are the number ferrite and martensite lattice sites with $N_F + N_M = N^2$, and K is the number of nearest neighbours of a lattice site with K_F and K_M occupied by ferrite and martensite, respectively, and $K_F + K_F = K$. The interfacial energy between ferrite and martensite is defined by J_{MF} while J_F, J_M and E_F, E_M are proportional to grain boundary energy and surface energy of ferrite and martensite, respectively. $\delta_{S_iS_j}$ (or $\delta_{Q_iQ_j}$, $\delta_{P_iP_j}$) is the Kronecker delta function with $\delta_{S_iS_j} = 1$ if $S_i = S_j$ where S_i (or S_j) indicate the type of phase ferrite (or martensite), Q_i (or Q_j) and P_i (or P_j) are the orientation indices of ferrite and martensite at sites i (or j), respectively.

Once the free energy of a lattice site is calculated, another random site is chosen and the free energy is calculated with the newly chosen crystallographic orientation. Depending on the change of energy, the new orientation is accepted with a probability index using Metropolis algorithm (Metropolis et al., 1953). The reorientation and grain growth takes place in instances when two randomly selected lattice sites (i.e. the initial site and one of its nearest neighbours) belong to the same ferrite or martensite phase, otherwise a site exchange is performed.

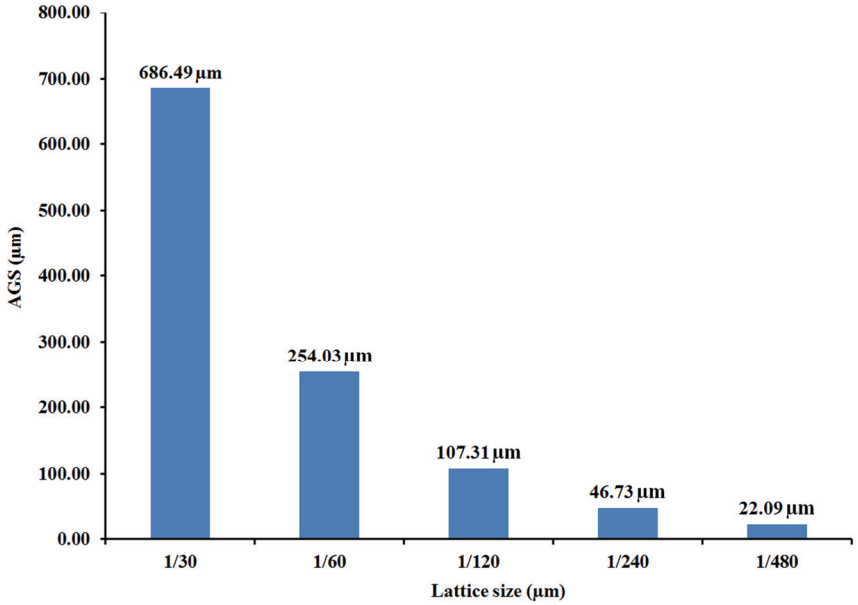

Fig. 3. *The predicted Average Grain Size (AGS) at the last Monte Carlo step based on varying initial lattice size.*

In this work, the grain growth procedure was carried out using 100 Monte Carlo steps to ensure a stabilised Average Grain Size (AGS) is achieved in the final microstructure. The AGS of each microstructure was directly related to the initial lattice size as shown in figure 3. Therefore, the lattice size, which is the only prescribed input parameter, is used throughout this work as a direct measure of AGS for each microstructure to study the effect of grain size variation. When the lattice size is varied, the volume fraction of martensite and ferrite in the final microstructure is dominated by the random state of the MC model. The predicted volume fractions of ferrite and martensite are shown in table 2. We assume that volume fractions of ferrite and martensite are kept constant when varying the lattice size since small variation of v_F and v_M for each different lattice size is less than 5% as shown in table 2.

Table 2. *Predicted volume fraction of ferrite and martensite at the end of Monte Carlo simulation by varying the initial lattice size parameter.*

	Lattice size (µm)				
	1/30	1/60	1/120	1/240	1/480
Volume fraction of ferrite (v_F)	0.66	0.62	0.65	0.67	0.62
Volume fraction of martensite (v_M)	0.34	0.38	0.35	0.33	0.38

The stabilised microstructures at the end of the last Monte Carlo simulation were used to generate finite element meshes of the simulated realistic micrographs. The heterogeneous elements were cut off at a threshold of 90% using an unconditional refinement. As such if an element had more than 10% heterogeneity it was refined into two separate elements of either four-node quadrilateral or three-node tetrahedral element.

The FE models were then imported into Abaqus 6.10 software package for processing. Definition of boundary conditions and material properties was carried out similar to the realistic microstructure-based RVE simulation described in the previous section. The whole procedure (MC modelling, meshing, processing and post-processing of the results) was automated using a python script to loop through various lattice sizes.

3. RESULTS AND DISCUSSION

Figure 4 shows the results of the RVE simulation as opposed to DIC experimental observations of Ghadbeigi et al. (2010). In the undeformed RVE simulation, the green (darker) areas are shown as ferrite and the red (lighter) regions are denoted as martensite. As an example, an initially undeformed grain of ferrite indicated by letter A in the DIC experiments are followed in both simulations and DIC observations. The elongated shapes of this grain is clearly captured and represented in the RVE simulations. In addition, the stress partitioning found with the RVE simulation is in strong agreement with the reported deformation mechanism of DP1000 steel by Ghadbeigi et al. (2010) in which both ferrite and martensite experience very similar average stresses and strain.

The inelastic strain and plastic stress distribution of each micrograph generated with varying lattice size in MC model is shown in figure 5. In the first column of this figure, the MC generated micrographs are shown with blue (dark) area being ferrite and the magenta (light) area representing martensite. The grain boundaries, identified by black colour in these micrographs are given same material properties similar to the ferrite. Clearly, the grain size and morphology of the phase distribution in these micrographs changes with varying the lattice size. For the

coarse grain size, with the lattice size of 1/30 μm, the large ferrite grains experience a low plastic stress, while near the grain boundaries the inelastic strain is at the highest in the ferrite grains. In this coarse grain case, the disparity of stress and strain distribution between ferrite and martensite is much more than micrographs with smaller grain size. Indeed, as the grain size reduces the flow of ferrite in between martensite islands becomes more apparent with the 45° shear bands clearly forming in the inelastic strain distribution.

with the previous works on stress partitioning between the soft and hard phases in a multiphase materials (Jacques et al., 2007). The effect of grain size is also shown in this figure for both phases with reference to the prescribed lattice size. When the lattice size increases from 1/30 to 1/480 μm, the grain size refines significantly too and the strengthening in both phases becomes apparent. With smaller grain size, the ductility of the ferrite and martensite phases reduces marginally as shown in figure 6. In addition, the lower stress levels reported in figure 6 compared

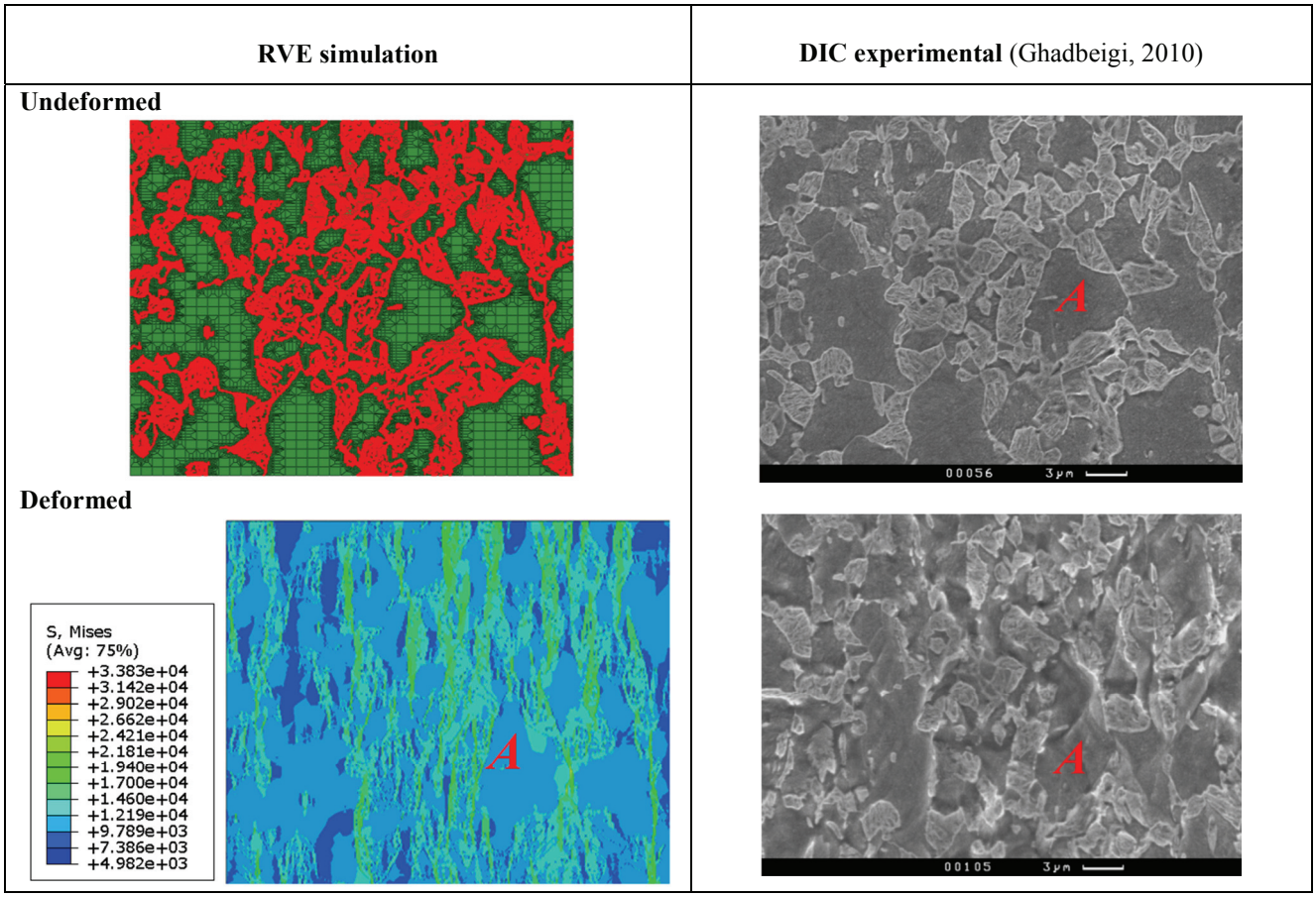

Fig. 4. *Plastic stress distribution in a deformed RVE simulation compared with the DIC experiments for the same micrograph (Ghadbeigi et al., 2010).*

In each of these cases, the per-phase distribution of stress and strain is calculated and plotted in figure 6. The calculation involves a volume averaged integral of all elements that belong to a specific phase, such that the values of stress or strain are summed over all integration points of these elements and divided by their total volume. This procedure is repeated for each phase independently. More detailed representation of the volume averaging process is given in Asgari et al. (2009). From data in this figure, it is clear that ferrite deforms to higher ductility at lower strengths while martensite undergoes lower deformation at higher strengths. This is consistent

to the input data in figure 1 is due the non-uniform distribution of stresses within the ferrite and martensite, also shown in figure 5. Within each phase, some areas are extremely stressed while other areas could be at lower stresses, and this consequently affects the volume averaging performed across each phase to obtain data in figure 6.

The slope of the tie line joining the stress-strain values of the two phases at each corresponding deformation state was determined as the parameter *m* shown in figure 1. Based on stress-strain partitioning shown in figure 6, the value of parameter *m* can be

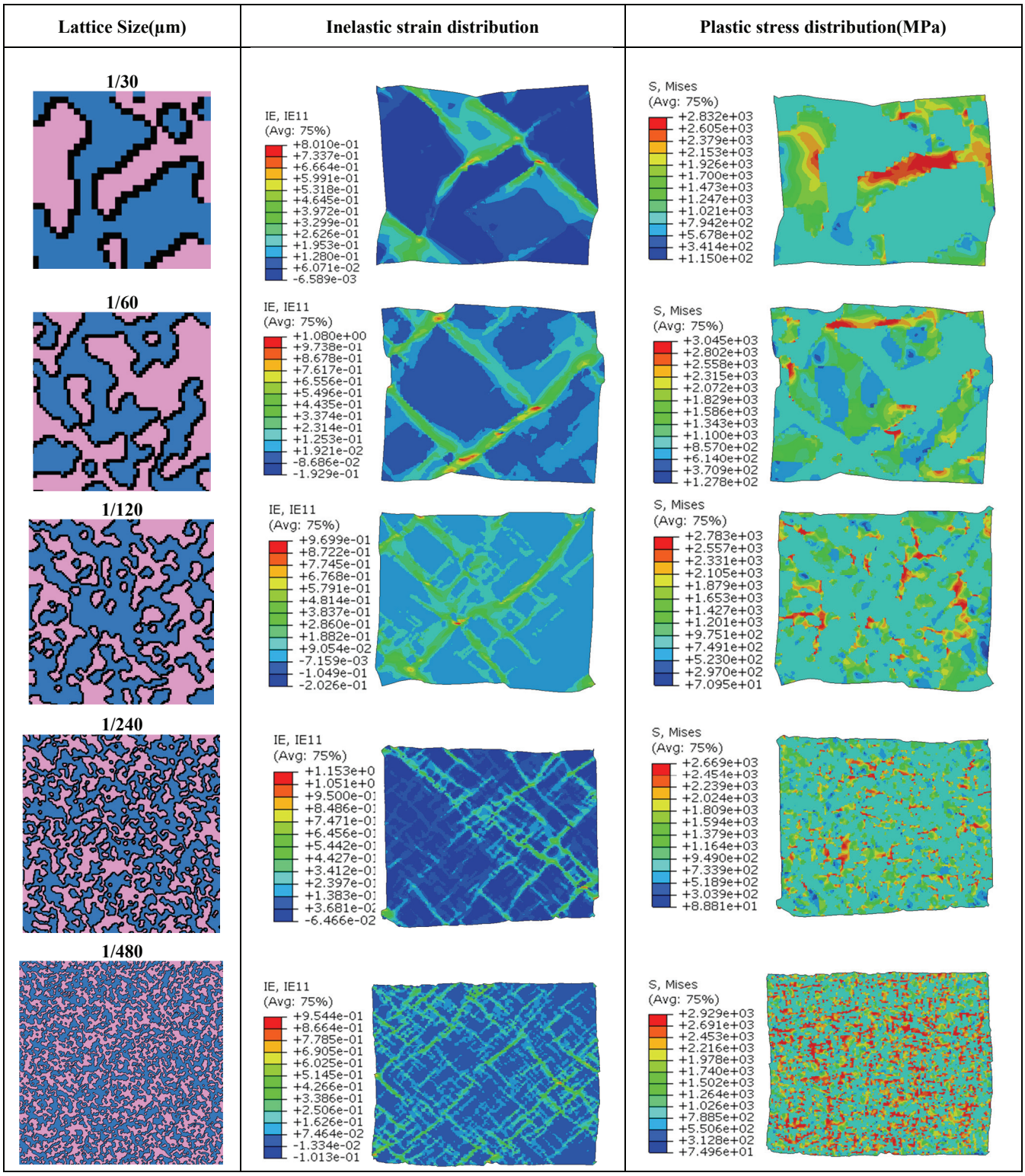

Fig. 5. *Inelastic strain and plastic stress localisation in microstructures of the same overall size generated with varying initial lattice size (proportional to the grain size) using Monte Carlo method.*

calculated for microstructures with varying lattice sizes and plotted in figure 7. It is interesting to note that after a certain level of straining in the microstructures, the value of m converges to 1 to 2 GPa regardless of the initial grain size. The effect of grain size is however very pronounced near the yield stress of the DP steel showing that the more grain size is refined, the higher is the slope of the line joining the state of stress between the two phases. In other words, sensitivity to phase morphology and grain size is much more pronounced during the yielding of the phases and the initial stages of the plastic localisation and as the material deforms the stress-strain partitioning of the steel converges to a state that is mainly dominated by factors other than the grain size and phase morphology.

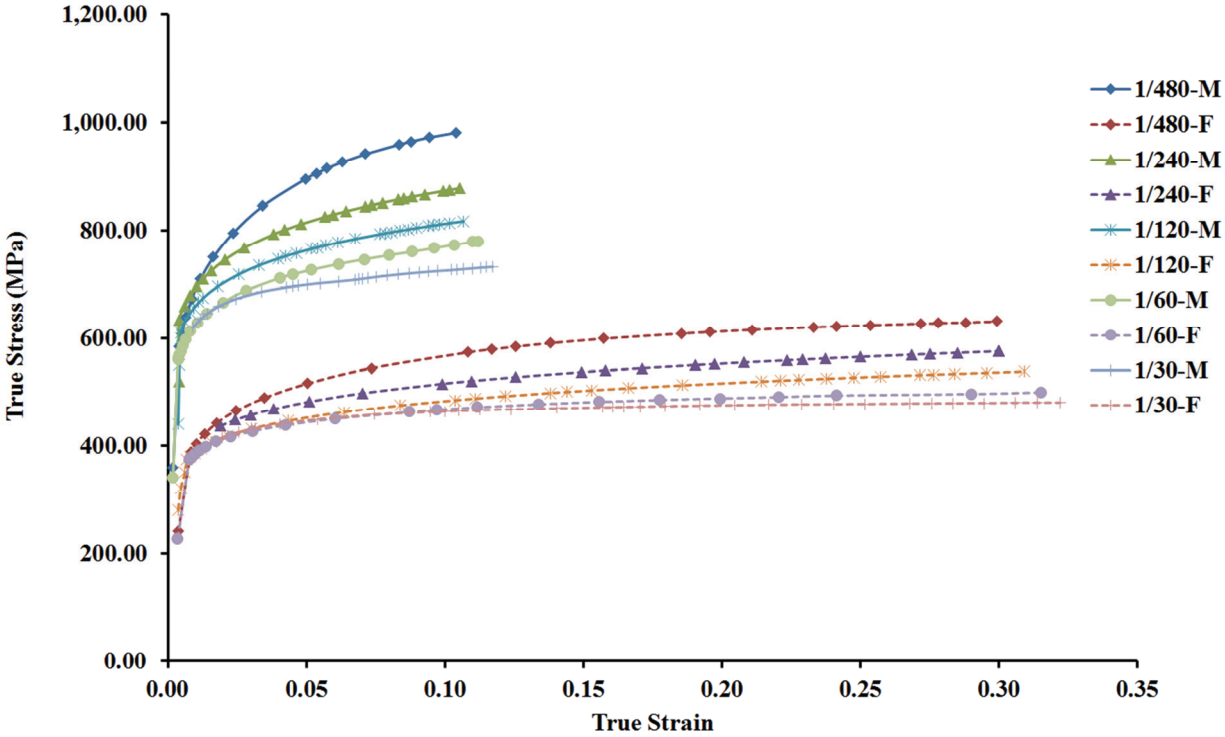

Fig. 6. *Microscale stress-strain partitioning between ferrite (F) and martensite (M) phases in microstructures with varying lattice parameters ranging from 1/30 μm to 1/480 μm.*

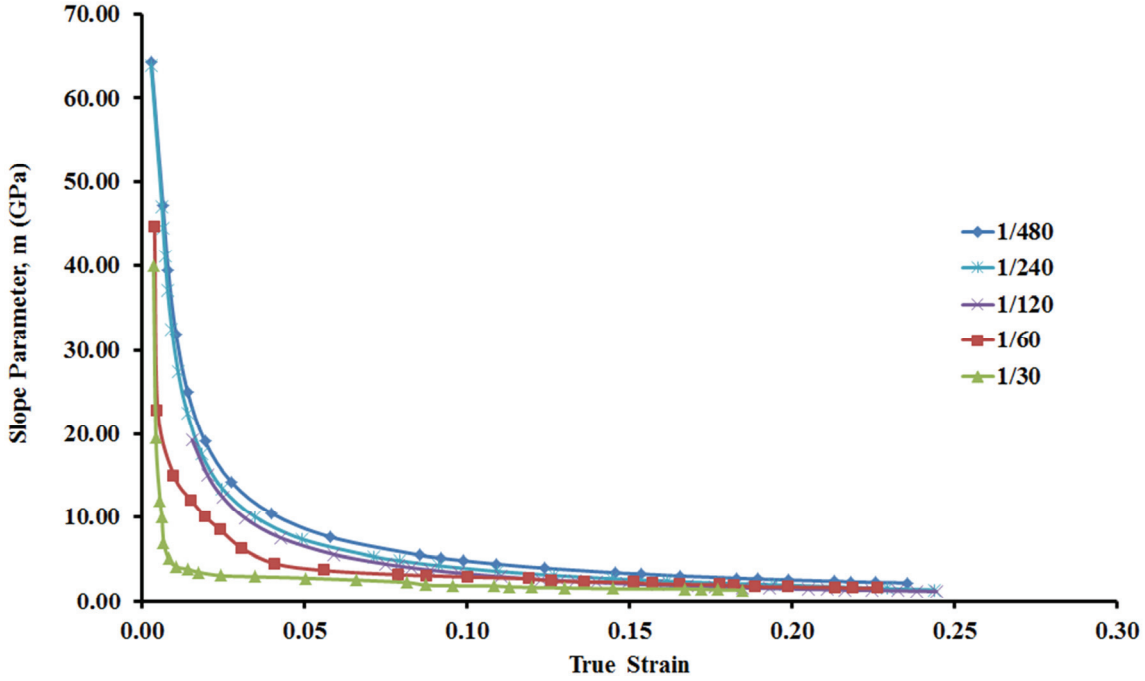

Fig. 7. *The slope parameter of the joining line between coressponding state of phases at microscale predicted using microstructures with varying lattice parameters ranging from 1/30 μm to 1/480 μm.*

The micromechanical solutions result in a macro stress-strain relationship for the DP590 steel, which is calculated during FE model and plotted in figure 8. The yield strength of this steel is expressed in its designation to be 590 MPa. The data in figure 8 shows that with increasing the grain size the predicted yield strength approaches the expected 590 MPa. The RVE model with 1/480 μm lattice size gives the most accurate account of this yield stress for DP590. This is consistent with the findings shown in figure 7 where the effect of grain size was significantly higher during the plastic localisation at the yield. How-

ever, from figure 8 it is clear that once the initial plastic localisation stage is passed the changes in the morphology and grain size variation has some noticeable effect on the strain hardening of the DP steel at higher strains. In these stages of deformation, an inverse relation of strain hardening to the grain size can be observed. The larger grain size model tends to behave similar to a perfectly-plastic material whereas the fine grain microstructures have higher strain hardening and toughness behaviour.

measured during Monte Carlo simulations (MCS) to generate the initial micrographs, followed by the image processing and meshing procedure (Meshing) and then processing and post-processing of the results using Abaqus software package (FE modelling). The total time spent for each simulation is the addition of all of these three steps for each microstructure lattice size. The most time consuming case was the refined microstructure with the 1/480 μm lattice size, which took nearly 45 minutes in total.

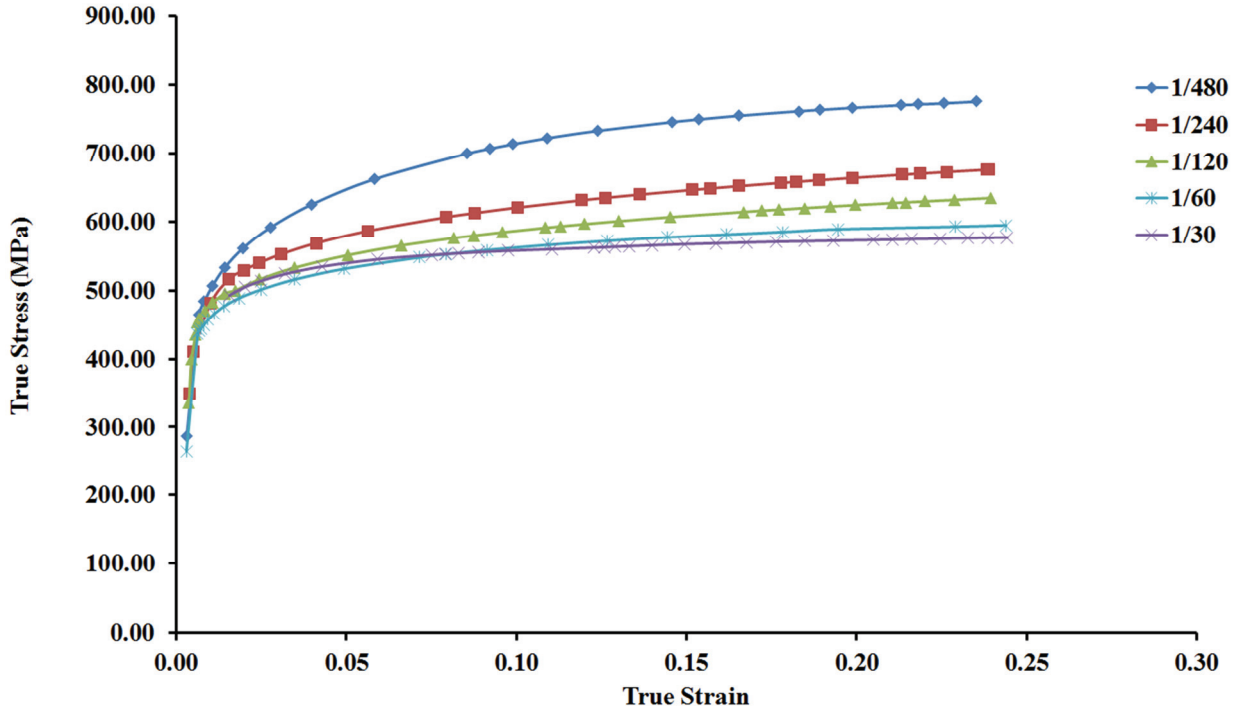

Fig. 8. *Macroscale homogenised flow curves predicted using microstructures with varying lattice parameters ranging from 1/30 μm to 1/480 μm.*

The stochastic modelling procedure of microstructures in this study was automated as it was described in the methodology section. The MC method is proven here to be a useful technique to generate microstructures that are relatively comparable to realistic microstructures and give the benefit that almost all parameters related to the microstructure morphology and grain size could be explicitly controlled during simulations. The MC method could directly output a digital microstructure that can be used as an RVE. In this work, however, an extra step is carried out where the digital microstructure of MC method is treated like an OM used earlier in this work for realistic microstructural models. This enables us to obtain microstructural meshes that are comparable between realistic and artificial MC-based microstructures. The cost of running simulations for different lattice sizes is shown in figure 9. The data presented here are the actual CPU time

This is clearly more efficient than actual experimental work to heat treat numerous samples to achieve multitude of grain sizes and phase morphologies of the DP steel. Furthermore, if the digital microstructure created from the MC method is meshed directly the cost of running multiple simulations could significantly decrease. Therefore, the MC method is suitable forthe multiscale modelling of DP steels in which the microstructure could be stochastically designed and tested virtually to establish the level of the stress and strain partitioning in the steel. It should be mentioned that using periodic boundary conditions is an essential component of maintaining representativeness of the RVE simulations as opposed to traction or displacement boundary conditions that have been used elsewhere (Sun, X. et al., 2009b).

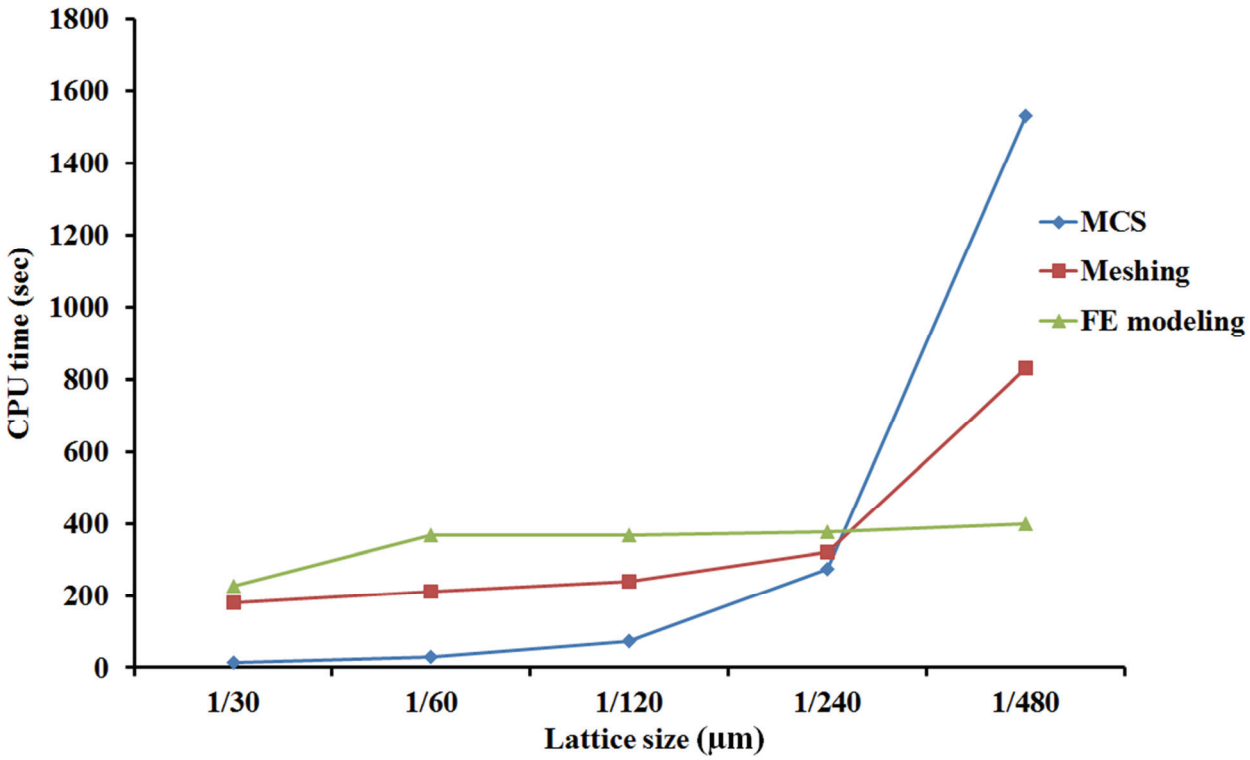

Fig. 9. *The cost of running simulations with varying lattice parameters defined in terms of CPU time spent on Monte Carlo simulations (MCS), digital image processing and mesh generation (Meshing) and finally, solution and post-processing of the RVEs using Abaqus software (FE modeling).*

4. CONCLUSIONS

This study set out to determine the effect of grain size and phase morphology in the realistic microstructure-based simulations of DP steels. The realistic microstructure-based model was used to compare the DIC observations on DP1000 steel with strong agreement in prediction of the stress and strain partitioning. In addition, the study has shown that by using Monte Carlo Potts model it is possible to create simulated micrographs of DP steel that resemble the realistic microstructure models of DP steel. The results of generating stochastic microstructures with MC Potts models show that average grain size of the microstructure could be controlled through a strong correlation with the initially prescribed lattice size parameter in the MC model. The resultant volume fractions of martensite and ferrite are shown to be almost constant with less than 5% variation. This enabled the possibility of assessing the effect of phase morphology and grain size in ductility and strength of DP steel. It was found that during initial local plastic deformation, the disparity of stress and strain partitioning is at the highest near the grain boundaries. The sensitivity of predictions to the level of stress and strain partitioning was determined to be highest near the yield stress of the DP steel while the refinement of the grain sizes gave a better prediction of the yield stress for the DP590 steel. The effect of grain size and phase morphology was found to be noticeable during strain hardening of DP steels with varying initial lattice sizes. A number of caveats need to be noted regarding the present study and similar works. The boundary conditions used in this study were prescribed as periodic BCs as opposed to traction and displacement BCs. In addition, complete bonding between ferrite and martensite phases were assumed during this work. In a more detailed future work, we will consider the effect of grain boundaries deformation by explicitly defining the corresponding grain boundary regions in between multiple phases. In addition, the possibility of using 3D stochastic microstructure modelling to carry out RVE modelling will be assessed to study the effect of triaxiality, grain volume size and microstructure morphology in multiphase materials such as DP steels.

Acknowledgment. The authors acknowledge the funding support from the Australian Research Council through the Laureate Fellowship award to Prof. P. D. Hodgson. The authors also thank Dr. Steven Celotto from Tata Steel Europe R&D for providing the material for this research.

REFERENCES

Al-Abbasi, F.M., Nemes, J.A. 2003, Micromechanical modeling of the effect of particle size difference in dual phase steels, *International Journal of Solids and Structures*, 40, 13-14, 3379-91.

Asgari, A., Hodgson, P.D., Rolfe, B.F. 2009, Modelling of Advanced High Strength Steels with the realistic microstructure-strength relationships, *Computational Materials Science*, 45, 4, 860-86.

Choi, K.S., Liu, W.N., Sun, X., Khaleel, M.A. 2009a, Influence of martensite mechanical properties on failure mode and ductility of dual-phase steels, *Metallurgical and Materials Transactions A*, 40A, 796-809.

Choi, K.S., Liu, W.N., Sun, X., Khaleel, M.A. 2009b, Microstructure-based constitutive modeling of TRIP steel: prediction of ductility and failure modes under different loading conditions, *Acta Materialia*, 57, 2592-604.

Choi, K.S., Soulami, A., Liu, W.N., Sun, X., Khaleel, M.A. 2010, Influence of various material design parameters on deformation behaviors of TRIP steels, *Computational Materials Science*, 50, 720-30.

Cong, Z.H., Jia, N., Sun, X., Ren, Y., Almer, J., Wang, Y.D. 2009, Stress and strain partitioning of ferrite and martensite during deformation, *Metallurgical and Materials Transactions A*, 40A, 1383-7.

De Cosmo, M., Galantucci, L.M., Tricarico, L. 1999, Design of process parameters for dual phase steel production with strip rolling using the finite-element method, *Journal of Materials Processing Technology*, 92-93, 486-93.

Delannay, L., Lani, F., Jacques, P. 2005, Simulation of deep-drawing of TRIP-assisted multiphase steel based on a micro-macro modelling, in *IDDRG2005*.

Dietrich, C., Poech, M.H., Fischmeister, H.F., Schmauder, S. 1993, Stress and strain partitioning in a Ag-Ni fibre composite under transverse loading, finite element modelling and experimental study, *Computational Materials Science*, 1, 195-202.

Ghadbeigi, H., Pinna, C., Celotto, S., Yates, J.R. 2010, Local plastic strain evolution in a high strength dual-phase steel, *Materials Science and Engineering A*, 527, 5026-32.

Hulka, K. 2003, Modern multi-phase steels for the automotive industry, *Materials Science Forum*, 414-415, 101-10.

Jacques, P.J., Furnemont, Q., Lani, F., Pardoen, T., Delannay, F. 2007, Multiscale mechanics of TRIP-assisted multiphase steels: I. Characterization and mechanical testing, *Acta Materialia*, 55, 3681-93.

Konieczny, A.A. 2001, On the formability assessment of the automotive Dual Phase steels, in *2001 World Congress, Society of Automotive Engineers*, 2001-01-3075, 1023-8.

Konieczny, A.A., Shi, M.F., Du, C. 2001, An experimental study of springback for Dual Phase steel and conventional High Strength Steel, in *International Body Engineering Conference (IBEC)*, Detroit, Michigan, 2001-01-3106, 1063-7.

Kouznetsova, V. 2002, *Computational homogenization for the multi-scale analysis of multi-phase materials*, PhD thesis, Eindhoven University of Technology.

Lani, F., Furnemont, Q., Jacques, P., Delannay, F., Pardoen, T. 2003, Micromechanical modeling of plastic anisotropy and strain induced phase transformation in dual-elastoplastic phase materials, *J. Phys. IV France*, 105, 139-47.

Lani, F., Furnemont, Q., Van Rompaey, T., Delannay, F., Jacques, P., Pardoen, T. 2007, Multiscale mechanics of TRIP-assisted multiphase steels: II. Micromechanical modelling, *Acta Materialia*, 55, 3695-705.

Metropolis, N., Rosenbluth, A.W., Rosenbluth, M.N., Teller, A.H., Teller, E. 1953, Equation and state calculations by fast computing machines, *The Journal of Chemical Physics*, 21, 2, 1087-92.

Ming Huang, C., Joanne, C.L., Patnaik, B.S.V., Jayaganthan, R. 2006, Monte Carlo simulation of grain growth in polycrystalline materials, *Applied Surface Science*, 252, 3997-4002.

Miodownik, M.A. 2002, A review of microstructural computer models used to simulate grain growth and recrystallisation in aluminium alloys, *Journal of Light Metals*, 2, 125-35.

Nikhare, C., Asgari, A., Weiss, M., Hodgson, P. 2010, Fracture of DP590 steel: a multiscale modeling approach, *Steel Research International*, 81, 9, 1450-3.

Nygards, M., Gudmundson, P. 2002, Micromechanical modeling of ferritic/pearlitic steels, *Materials Science and Engineering A*, 325, 435-43.

Rashid, M.S. 1981, Dual Phase steels, *Ann. Rev. Mater. Sci.*, 11, 245-66.

Saleh, M.H., Priestner, R. 2001, Retained austenite in dual-phase silicon steels and its effect on mechanical properties, *Journal of Materials Processing Technology*, 113, 1-3, 587-93.

Soulami, A., Choi, K.S., Liu, W.N., Sun, X., Khaleel, M.A., Ren, Y., Wang, Y.D. 2010, Predicting fracture toughness of TRIP 800 using phase properties characterized by In-Situ High Energy X-Ray Diffraction, *Metallurgical and Materials Transactions A*, 41A, 1261-8.

Soulami, A., Choi, K.S., Shen, Y.F., Liu, W.N., Khaleel, M.A. 2011, On deformation twinning in a 17.5% Mn-Twip steel: A physically based phenomenological model, *Materials Science and Engineering A*, 528, 1402-8.

Sun, X., Choi, K.S., Liu, W.N., Khaleel, M.A. 2009a, Predicting failure modes and ductility of dual phase steels using plastic strain localization, *International Journal of Plasticity*, 25, 1888-909.

Sun, X., Choi, K.S., Soulami, W.N., Liu, W.N., Khaleel, M.A. 2009b, On key factors influencing ductile fractures of dual phase (DP) steels, *Materials Science and Engineering A*, 526, 140-9.

Terada, K., Hori, M., Kyoya, T., Kikuchi, N. 2000, Simulation of the multi-scale convergence in computational homogenization approaches, *International Journal of Solids and Structures*, 37, 2285-311.

Van der Sluis, O., Schreurs, P.J.G., Brekelmans, W.A.M., Meijer, H.E.H. 2000, Overall behaviour of heterogeneous elastoviscoplastic materials: effect of microstructural modelling, *Mechanics of Materials*, 32, 449-62.

Wagoner, R.H. 2006, Advanced High Strength Steels: Fundamental Research Issues, Accessed online (June 2007) at http://www.a-sp.org/nsf/index.htm, in *NSF Workshop*, Arlington, VA, USA.

Zaefferer, S., Ohlert, J., Bleck, W. 2004, A study of microstructure, transformation mechanisms and correlation between microstructure and mechanical

properties of a low alloyed TRIP steel, *Acta Materialia*, 52, 2765-78.

Zheng, Y.G., Lu, C., Mai, Y.M., Gu, Y.X., Zhang, H.W., Chen, Z. 2006, Monte Carlo simulation of grain growth in two-phase nanocrystalline materials, *Applied Physics Letters*, 88, 144101-3.

WIELOSKALOWE MODELOWANIE ROZDZIAŁU NAPRĘŻEŃ I ODKSZTAŁCEŃ W STALACH DWUFAZOWYCH O WYSOKIEJ WYTRZYMAŁOŚCI.

Streszczenie

Wieloskalowe modelowanie rozdziału naprężeń i odkształceń w stalach dwufazowych (DP) przeprowadzono wykorzystując zarówno reprezentatywny element objętości (ang. representative volume element – RVE) z rzeczywistą mikrostrukturą jak i stochastyczną mikrostrukturę wygenerowaną metodą Monte Carlo. Stochastycznie wygenerowane mikrostruktury przypominały te rzeczywiste, umożliwiając badanie specyficznych cech mikrostruktury trudnych do analizowania metodami doświadczalnymi. Jedną z takich cech była wielkość ziarna i morfologia ziaren. Mikrostruktury wygenerowano stosując różne średnie wielkości ziarna podczas gdy pozostałe parametry, takie jak warunki brzegowe, własności materiału oraz ułamek objętości martenzytu i ferrytu pozostawały niezmienione. W konsekwencji zaobserwowano, że wpływ wielkości ziarna jest bardzie widoczny w czasie inicjalizacji lokalizacji odkształcenia plastycznego oraz wokół powierzchni międzyfazowych. Dodatkowo stwierdzono, że spadek plastyczności i wzrost wytrzymałości stali DP są związane z rozdrobnieniem ziarna każdej z faz oraz z rozdziałem naprężeń i odkształceń między fazami.

Received: August 23, 2012
Received in a revised form: December 6, 2012
Accepted: December 18, 2012